

Nucleation and Growth of Nonclassical Droplets

Dieter W. Heermann and W. Klein

Center for Polymer Studies and Department of Physics, Boston University, Boston, Massachusetts 02215

(Received 12 October 1982)

Nucleation and growth are studied in the metastable region of the Glauber-kinetic Ising model with medium-range interactions. Monte Carlo data indicate that the nucleating droplets are not in general compact but quickly become so during the initial phase of growth and then grow as compact droplets. This two-stage growth process is also predicted by a qualitative theory.

PACS numbers: 64.60.My, 05.20.-y, 05.70.Jk

Previous Monte Carlo simulations of the nucleation and growth processes in Ising models have focused on systems with short-range interactions.¹⁻⁴ These studies have indicated that away from the critical point the nucleating droplets are quite compact and that classical nucleation and growth theory⁵⁻⁷ accurately describes the phenomenon. However, studies^{8,9} of the properties of the metastable states of Ising models with medium-range interactions and Glauber kinetics have indicated that the "equilibrium" droplet distribution was not that of a classical droplet model for deep quenches, but was of a ramified or lattice-animal¹⁰ form. In this Letter we report the results of Monte Carlo simulations of the nucleation and growth phase of these medium-range models and also present a "zeroth-order" theory which gives some qualitative understanding of the data.

In our simulations we used the equivalent-neighbor model¹¹ for a simple cubic lattice of size 40^3 . In this model each spin interacts with any spin within the interaction range R_I , i.e., with q neighbors (here $q=124$). Within R_I the interaction energy is constant and there is no interaction with spins outside the range R_I . We worked at $T/T_c \approx 0.45$, where T_c is the critical temperature of this model. The effective magnetic field $h = 2 \times (\text{magnetic dipole moment}) \times (\text{magnetic field}) / k_B T$ was fixed at $h = 1.35$. (The mean-field spinodal is at $h_s = 1.42$.) We started with a totally ordered configuration. The magnetic field was then turned on in the direction opposite to the magnetization. With use of Glauber kinetics and random selection of spins, the system was monitored as it evolved into metastable equilibrium and then nucleated. During this time, configurations were periodically frozen and analyzed.

The primary results of our simulations are contained in Fig. 1 where $\ln S$ is plotted against $\ln R$. Here S is the number of spins in a droplet and R

is its radius of gyration defined by $R^2 = (1/S) \sum_i r_i^2$. Note that we have used the metric $\max(\Delta x, \Delta y) \approx R_I$ for the interaction and the Euclidean metric for the radius of gyration. Our droplets are defined with percolation concepts, i.e., two up spins are said to belong to the same droplet (or cluster) if they are closer together than the interaction range and if there is an active bond between them. Bonds between up spins are active with a probability $p_b = 1 - \exp[(-4J/k_B T)(1 - \rho)]$, where ρ is the density. The reasons for choosing

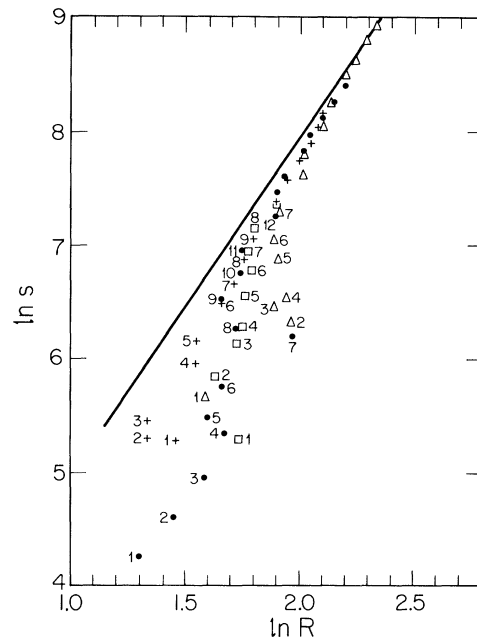


FIG. 1. Logarithm of the cluster size S vs logarithm of the radius of gyration R of the droplet. Different symbols denote separate runs and the numbering indicates time sequence with number 1 being the nucleating droplet. For simplicity, four runs are shown that represent 20% of the data taken. The four sets represent the two extreme cases of the most compact and the most ramified nucleating droplets and two intermediate cases.

such a definition for droplets is discussed elsewhere.^{9,12} Here we simply mention that we have numerically verified the predictions based on this droplet definition for the quasiequilibrium properties in the metastable state.⁹ In Fig. 1 each type of symbol represents a different Monte Carlo run and the points are numbered in time sequence with number 1 in each run being the best guess for the nucleating droplet. Two criteria were used to determine the onset of nucleation; at least one droplet grew monotonically and the magnetization increased monotonically until the stable phase was reached. Two points should be noted. (1) There is a large spread in the size of the nucleating droplet when measured by either S or R , i.e., there is no well-defined critical size. This is in contrast to the predictions of classical nucleation theory. (2) Inspection of Fig. 1 indicates that the droplets grow in two stages. In the initial stage R remains roughly constant. In the later stage the growth can be fitted by a straight line with slope 3 in agreement with classical theory.

A useful concept for analyzing the data is the effective dimension $d_+ \equiv \ln S / \ln R$. This is to be distinguished from the fractal dimension¹³ $d_f \equiv -\ln A / \ln R + \ln S / \ln R$, where A is an amplitude that is bounded but may depend on R . Clearly in the limit $R \rightarrow \infty$, $d_+ = d_f$; however, for finite R , $d_+ = d_f + \ln A / \ln R$. The concept of effective dimension is useful for finite R , when A is not constant, because it is impossible to separate the effects of d_f and A . In the later stage of growth where the data can be fitted with a straight line with slope 3, we have $d_+ = 3 + C / \ln R$, where C is the intercept of the $\ln S$ vs $\ln R$ plot at $\ln R = 0$.

The data in Fig. 1 can now be interpreted in the following way: Initially, the droplet that causes nucleation of the system generally has $d_+ < 3 + C / \ln R$. During the initial stage of growth R remains constant while the droplet fills in or "compactifies" until $d_+ = 3 + C / \ln R$. The droplet then grows according to the classical growth theory. We will call droplets with $d_+ = 3 + C / \ln R$ compact and droplets with $d_+ < 3 + C / \ln R$ ramified.

It is also important to note that the spread in the $\ln S$ vs $\ln R$ plot which occurs at nucleation decreases as a function of time. Here we should mention that the data in Fig. 1 represent 20% of the data taken. The remaining data are consistent with that shown in the figure and were omitted for the sake of clarity of the diagram. This is consistent with our interpretation of compactification in the initial growth state and suggests

that it takes place in a finite, rather short, time. We can understand some of the features of the data by means of a very simple theory described below.

In previous theories of cluster growth^{12,14} droplets are assumed to be compact and the only significant addition of monomers takes place on the surface. Consequently each additional monomer contributes to the growth of the droplet radius. For more ramified droplets additional monomers can add to either the growth of the radius or the effective dimension d_+ of the droplet. Moreover these two processes can compete with each other for the available monomers in the environment of the droplet.

In most considerations of droplet growth it is assumed that the difference between the capture and the evaporation rates after nucleation is proportional to the droplet surface,¹⁵ which for ramified droplets would not be proportional¹⁶ to $S^{(d-3)/d}$. We should also take into account the possible screening of surface sites by the proximity of other occupied sites.¹⁷ In order to account for these effects we will divide the ramified droplet of S spins into two parts (see Fig. 2) by means of two concentric spheres whose centers are at the center of mass of the droplet. The outer sphere (1) is the smallest sphere that contains the entire droplet. The spins in the inner sphere we will designate as the interior of the droplet and the spins in the shell between spheres 1 and 2 we will call the exterior. The number of spins in the two regions will be designated as S_I and S_E , respectively. On physical grounds we argue that the effective surface, i.e., the surface available for the incorporation of monomers after screening is accounted for, is different in these two regions. The exterior shell is envisioned as quite small compared with the interior and plays the role of an outer "surface." We define screening parameters x and y ($x, y \leq 1$) by taking for the

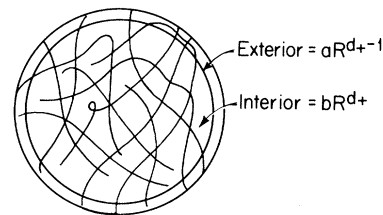


FIG. 2. Schematic ramified droplet with two concentric spheres dividing the droplet into an interior and exterior region. For low temperatures the droplet is more cubical.

effective interior and exterior surfaces S_I^x and S_E^y , respectively. With the assumption that the difference between capture and evaporation rates is proportional to the effective surface, we have

$$dS_I/dt = \alpha S_I^x, \quad (1)$$

and

$$dS_E/dt = \beta S_E^y, \quad (2)$$

where α and β may depend on x and y but for simplicity will be considered, as with x and y ,

independent of time. We complete our formulation by taking

$$S_E = aR^{d_+ - 1}, \quad (3)$$

and

$$S_I = bR^{d_+}, \quad (4)$$

where a and b are constants. Since R^{d_+} will be large for all t after nucleation, the equations to first order in t will be a good approximation to the solutions of Eqs. (1)–(4). We obtain

$$\ln R = \ln R^* + \alpha t / (1 - y)(R^*)^{d_+^*(1-y)} - \beta t / (1 - x)(R^*)^{(d_+^* - 1)(1-x)}, \quad (5)$$

and

$$d_+ = d_+^* + t / \ln R [\alpha(1 - d_+^*) / (1 - y) + d_+^* \beta / (1 - x)], \quad (6)$$

where quantities with asterisks are the values at $t=0$.

Equations (5) and (6) allow a qualitative understanding of Fig. 1. If we set $d_+ = 3 + C / \ln R$ in Eq. (5) we obtain t_c , the time that it takes for the droplet to compactify:

$$t_c = [\ln R^* (d - d_+^*) - C] \{ [\alpha(1 - d_+^*) / (1 - y) + d_+^* \beta / (1 - x)] + [\alpha / (1 - y)(R^*)^{d_+^*(1-y)} - \beta / (1 - x)(R^*)^{(d_+^* - 1)(1-x)}] \}^{-1}. \quad (7)$$

Over this time interval the growth in R is given by

$$\ln R = \ln R^* + \ln R^* [D_1 / (R^*)^{d_+^*(1-y)} + D_2 / (R^*)^{(d_+^* - 1)(1-x)}], \quad (8)$$

where D_1 and D_2 are constants that depend on α , β , x , y , d_+^* , and R^* . Equations (7) and (8) predict that for finite R^* the droplet will compactify in a finite time and that during this time the change in R will be small since

$$\ln R^* / (R^*)^{d_+^*(1-y)}$$

will be a small quantity.

It is interesting to note that Eqs. (7) and (8) also predict that t_c will diverge as $\ln R^*$ as we get closer to the mean-field spinodal where R^* diverges.¹⁸ This limit will produce an even smaller increase in R over the t_c time interval.

Finally it should be noted that Eqs. (5) and (6) indicate the possibility of other forms of "growth" after nucleation. For example, Eqs. (5) and (6) admit solutions where d_+ increases while R decreases for $\alpha/\beta \gg 1$ and where d_+ decreases and R increases for $\alpha/\beta \ll 1$. The physical content of these growth patterns and their possible connection with effects observed in deep quenches¹⁹ is being investigated.

To summarize, we have performed Monte Carlo simulations on Ising models with medium-range interactions and found evidence to support the interpretation that in deep quenches the nucleating droplets²⁰ are in general noncompact. This is consistent with the result that critical droplet

surfaces become diffuse in the limit of large R .¹⁸ These droplets grow by rapidly compactifying and then growing as compact droplets. We have also presented a crude theory that gives results consistent with this interpretation.

We would like to acknowledge interesting and useful conversations with D. Stauffer and A. Coniglio. This work was supported in part by grants from the U. S. Army Research Office, the U. S. Office of Naval Research, and the National Science Foundation.

¹K. Binder, *Ann. Phys. (N.Y.)* **98**, 390 (1976).

²M. Kalos, J. L. Lebowitz, O. Penrose, and A. Sur, *J. Stat. Phys.* **18**, 39 (1978).

³D. Stauffer, A. Coniglio, and D. W. Heermann, *Phys. Rev. Lett.* **49**, 1299 (1982).

⁴K. Binder and M. H. Kalos, *J. Stat. Phys.* **22**, 363 (1980).

⁵W. I. Goldberg, in *Scattering Techniques Applied to Supramolecular and Nonequilibrium Systems*, edited by S. H. Chen, B. Chu, and R. Nossal (Plenum, New York, 1981).

⁶C. S. Kiang, D. Stauffer, G. H. Walker, O. P. Puri, J. D. Wise, and E. M. Patterson, *J. Atmos. Sci.* **28**,

1222 (1971).

⁷See also the articles in *Nucleation*, edited by A. C. Zettlemoyer (Marcel Dekker, New York, 1969).

⁸D. W. Heermann, W. Klein, and D. Stauffer, *Phys. Rev. Lett.* **49**, 1262 (1982).

⁹D. W. Heermann and W. Klein, *Phys. Rev. B* **27**, 1732 (1983).

¹⁰W. Klein, *Phys. Rev. Lett.* **47**, 1569 (1981).

¹¹C. Domb and H. W. Dalton, *Proc. Phys. Soc. London* **89**, 859 (1966).

¹²D. W. Heermann, A. Coniglio, W. Klein, and D. Stauffer, to be published.

¹³B. B. Mandelbrot, *Fractals: Form, Chance, and*

Dimension (Freeman, San Francisco, 1977); H. E. Stanley, *J. Phys. A* **10**, L211 (1977).

¹⁴I. M. Lifshitz and V. V. Slyozov, *J. Phys. Chem. Solids* **19**, 35 (1961).

¹⁵See the review by J. D. Gunton, M. San Miguel, and P. S. Sahni, to be published.

¹⁶D. Stauffer, *Phys. Rep.* **54**, 1 (1979); A. Coniglio, private communication.

¹⁷P. A. Rikvold, *Phys. Rev. A* **26**, 647 (1982).

¹⁸J. S. Langer, *Ann. Phys. (N.Y.)* **41**, 108 (1967).

¹⁹K. Binder, *Solid State Commun.* **34**, 191 (1980).

²⁰A detailed discussion of why this decay process is nucleation will be presented in a future publication.